Optica Imaging Congress (3D, COSI, DH, FLatOptics, IS, pcAOP) © Optica Publishing Group 2023

Accurate and Fast Phase Compensation of Dynamic Samples in Digital Holographic Microscopy

Sofía Obando-Vásquez[1], Ana Doblas[2] and Carlos Trujillo[1]
[1]*Applied Optics Group, School of Applied Science and Engineering, Universidad EAFIT, Medellín, Colombia*
[2]*Department of Electrical and Computer Engineering, The University of Memphis, TN, USA*
SOV: sobandov@eafit.edu.co AD: adoblas@memphis.edu CT: catrujilla@eafit.edu.co

Abstract: We present a fast algorithm for accurate phase compensation of holographic videos of dynamic phenomena recorded in a digital holographic microscope. The proposal is tested with human sperm and red blood cell samples. © 2023 The Author(s)

1. Introduction

Digital holographic microscopy (DHM) is an imaging technique for recovering the complex wavefield scattered by microscopic samples from their interferograms registered with a digital sensor without staining or fixation procedures [1]. Under off-axis configuration, DHM offers single-shot amplitude and phase information reconstructions, making it a particularly attractive technique for studying dynamic biological samples [2]. The main challenge in this configuration is generating a numerical reference wavefront that compensates the *xy*-tilting angle between the interfering waves that reach the detector. Traditionally, grid-search algorithms have been proposed for estimating the numerical reference's parameters [3]. Although these algorithms are accurate, they have high computational complexity. Heuristic algorithms [4] have been proposed to alleviate the high computational complexity. Nevertheless, these algorithms are still limited, as the phase background level may occasionally change within the reconstruction of hologram stacks. To address these challenges, we propose an efficient algorithm capable of quickly recovering compensated phase map images from a stack of holograms with minimum background level changes and high accuracy in the reconstructions at six frames per second for images of 1280x960 pixels. This technique considers that the compensating spatial frequencies between successive frames in the Fourier domain of the holograms are located in a sub-pixel region. As a result, after the second frame of the holographic video, the only requirement for accurate phase compensation is an efficient fine-tuning of these parameters. This proposal is validated with two experimental biological samples: smeared red blood cells and human sperm.

2. Phase compensation algorithm

In some biological applications, it is desirable to study the behavior of a living organism and its evolution [5]. For this, one must have algorithms capable of quickly recovering phase map images from a stack of holograms with minimum background level changes [6]. Our proposed algorithm utilizes a nested-search approach to find the carrier spatial frequencies of holograms recorded in telecentric-off-axis mode [7]. This mode corrects the spherical phase aberration resulting from the microscope objective (MO) by inserting a tube lens (TL) and creating a *4f-like* system between the components. This physical arrangement leaves only the phase aberration caused by the *xy*-tilting angle between the off-axis interfering waves to be addressed. The algorithm compensates for this linear phase aberration by producing a numerical reference wavefront described mathematically in equation (1).

$$r_D(m\Delta x, n\Delta y) = \exp\left[ik\left(m\Delta x \sin\theta_x + n\Delta y \sin\theta_y\right)\right]. \quad (1)$$

In equation (1), $k = 2\pi/\lambda$ is the wave number being λ the source's wavelength, (m, n) are whole numbers accounting for the location in the image plane, $(\Delta x, \Delta y)$ are the pixel pitch in each dimension, and (θ_x, θ_y) are the tilting angles between the wavefront vector of the interfering wavefronts at the sensor plane. Equation (2) fully describes these angles:

$$\theta_x = \sin^{-1}\left(\left(\frac{M}{2} - f_x\right)\frac{\lambda}{M\Delta x}\right), \qquad \theta_y = \sin^{-1}\left(\left(\frac{N}{2} - f_y\right)\frac{\lambda}{N\Delta y}\right). \quad (2)$$

In equation (2), (M, N) are the hologram size in pixels along the horizontal and vertical direction, respectively, and (f_x, f_y) are the carrier spatial frequencies of the +1 diffraction term. When point-wise multiplying the spatially filtered +1diffraction order of the hologram by equation (1), one can remove the linear phase factor due to the tilting angle between interfering waves, allowing the retrieval of the sample's phase and amplitude information from a single

hologram recording provided this angle is accurately selected. Therefore, the goal of the compensation algorithms is to estimate accurately (f_x, f_y).

Our proposal uses a nested search around the +1 diffraction order to calculate these spatial frequency coordinates, as shown in Figure 1 a). Each mesh has a dimension of 2(*G*step*) pixels, as depicted in that figure. For the first frame of the video, these two parameters have been calibrated to $G = 3$ and $step = 0.5$. Then, the iterative nested-search process depicted in Figure 1 b) is executed to estimate the carrier frequency of the first frame ($f_{x\,out}$, $f_{y\,out}$ represented as the blue circle in panel b). Then, for the next hologram of the stack, $f_{x\,out}$ and $f_{y\,out}$ are located in the upper right corner of the first mesh of the algorithm (red mesh in Figure 1 b)). For this frame, the mesh size is significantly smaller due to the correlation between consecutive frames; therefore, the mesh parameters are set to $G = 0.2$ and $step = 0.1$. The shrinkage in the first mesh (i.e., $G = 0.2$ instead of $G = 3$) is crucial for reducing the compensation times. This process generates compensated phase maps at rates that allow dynamic phenomena visualization. For the experimental validation of the proposal, we recorded two holographic videos in a digital holographic microscope in an off-axis telecentric configuration. The first sample was a smearing of human red blood cells (RBCs), and the second was human sperm.

To validate the performance of the reconstruction in the holographic stack, we measured a mean slope over the phase map image, as shown in panel c): take the profile over the color lines depicted in that figure and take the mean value of the slopes of these profiles. When this mean value is near 0, we ensure the algorithm is recovering a flat phase map, i.e., a fully compensated phase measurement. Additionally, we measure the compensation time for executing the reconstruction of each phase map. In panels f) and i), we present three reconstructions of frames of each holographic video. In panels d) and g), we report the compensation times for the RBC and the human sperm's video processed in a computer station powered by an Intel(R) Xenon(R) running at 3.60 GHz. From them, we can conclude that our algorithm has good stability in the reconstruction times, compensating video frames at rates of 5 and 6 fps, respectively. Finally, panels e) and h) present the mean slope value for each frame. As one can note, our algorithm has high accuracy since all reconstructed frames have a slope whose order of magnitude is between 10^{-3} ~10^{-4} radians.

This study empirically validates an accurate and stable phase compensation algorithm using two holographic videos of human red blood cells (RBCs) and human sperm. The reconstruction performance has been measured using the mean slope over the phase map images. The results demonstrate that the proposed algorithm has high accuracy, recovering a flat phase map with a fully compensated phase measurement at up to 6 fps for the studied dynamic samples.

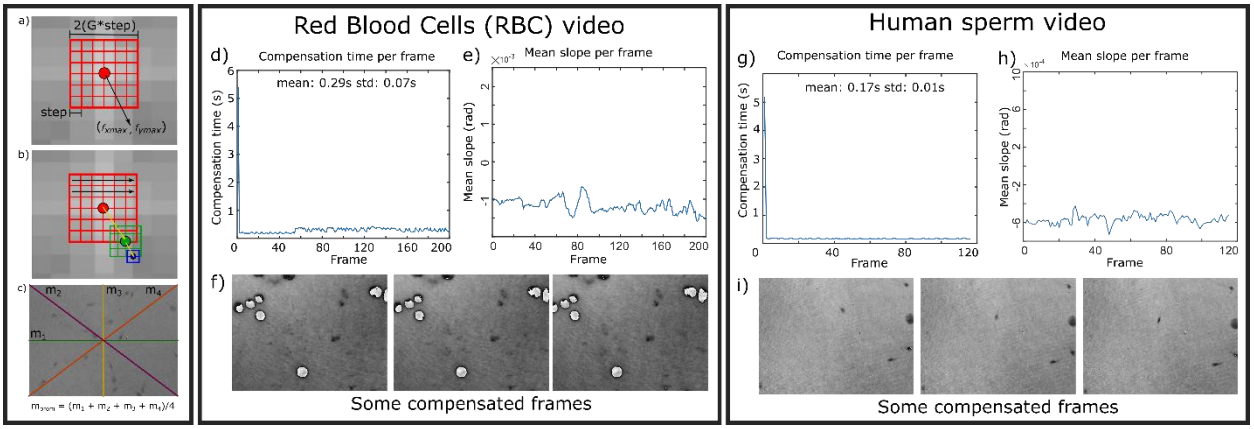

Fig. 1 Schematic description of the proposed algorithm and results: a). Parameters of the search mesh, b) Nested-search procedure graphic description. The black arrow corresponds to the evaluation direction of the mesh; c) Profiles for the mean slope calculation; d) and g) Plots of the compensation times for each frame of the RBC and the human sperm holographic videos, respectively; e) and h) mean slope per frame for the RBC and the human sperm respectively and f) and i) extract of three frames of each holographic video.

3. References

[1] M. K. Kim, Springer Series in Optical Sciences 162, 149 (2011).
[2] B. Kemper and G. von Bally, Appl Opt 47, A52 (2008).
[3] R. Castaneda, C. Trujillo, and A. Doblas, Sensors 21, 8021 (2021).
[4] R. Castaneda and A. Doblas, Applied Optics, Vol. 60, Issue 32, pp. 10214-10220 60, 10214 (2021).
[5] A. Anand, V. K. Chhaniwal, and B. Javidi, Journal of Display Technology, Vol. 6, Issue 10, pp. 500-505 6, 500 (2010).
[6] R. Castaneda, C. Trujillo, and A. Doblas, Sensors, vol. 21, no. 23, pp. 8021, (2021).
[7] E. Sánchez-Ortiga, P. Ferraro, M. Martínez-Corral, G. Saavedra, and A. Doblas, Journal of the Optical Society of America A 28, 1410 (2011).